




Article

Potentially Toxic Elements in Oasis Agricultural Soils Caused by High-Intensity Exploitation in the Piedmont Zone of the Tianshan Mountains, China

Wen Liu ^{1,2,3} , Long Ma ^{1,2,3,*}  and Jilili Abuduwaili ^{1,2,3} 

- ¹ State Key Laboratory of Desert and Oasis Ecology, Xinjiang Institute of Ecology and Geography, Chinese Academy of Sciences, Urumqi 830011, China; liuwen@ms.xjb.ac.cn (W.L.); jilil@ms.xjb.ac.cn (J.A.)
- ² Research Center for Ecology and Environment of Central Asia, Chinese Academy of Sciences, Urumqi 830011, China
- ³ College of Resources and Environment, University of Chinese Academy of Sciences, Beijing 100049, China
- * Correspondence: malong@ms.xjb.ac.cn

Abstract: Considering the pollution of potentially toxic elements (PTEs) in the soils of China, the present study analyzed the current state and influencing factors of PTEs in oasis soils using the model of absolute principal component score–multiple linear regression in the piedmont zone of the Tianshan Mountains. The possible non-carcinogenic and carcinogenic risks of PTEs at current concentrations were also explored using a human-health risk-assessment model. The results suggested that the extent to which potentially toxic elements in the soils of different geographical units in the study area is affected by human activities varies considerably. The PTEs Cd and As in the soils of the Yili River Watershed were the most strongly influenced by human activities, reaching levels of 40% and 59%, respectively. However, in the Bortala River Watershed, Cu, Cd, and As were the most strongly influenced by human activities, reaching levels of 33%, 64%, and 76%, respectively. Geographical units with a high degree of economic development (e.g., the Yili River Watershed) had, in contrast, low levels of PTE pollution caused by human activities, which may be related to the regional economic development structure. The human health risk assessment showed that the non-carcinogenic and carcinogenic risks of PTEs are currently below the threshold. However, increasing the arsenic content to 1.78 times the current level in the Bortala River Watershed would lead to carcinogenic risk. For the Yili River Watershed, a 3.33-fold increase in the arsenic content above its current level would lead to a carcinogenic risk. This risk should be addressed, and targeted environmental-protection measures should be formulated. The present research results will provide important decision support for regional environmental protection.



Citation: Liu, W.; Ma, L.; Abuduwaili, J. Potentially Toxic Elements in Oasis Agricultural Soils Caused by High-Intensity Exploitation in the Piedmont Zone of the Tianshan Mountains, China. *Agriculture* **2021**, *11*, 1234. <https://doi.org/10.3390/agriculture11121234>

Academic Editor: Fernando P. Carvalho

Received: 13 November 2021
Accepted: 6 December 2021
Published: 7 December 2021

Publisher's Note: MDPI stays neutral with regard to jurisdictional claims in published maps and institutional affiliations.



Copyright: © 2021 by the authors. Licensee MDPI, Basel, Switzerland. This article is an open access article distributed under the terms and conditions of the Creative Commons Attribution (CC BY) license (<https://creativecommons.org/licenses/by/4.0/>).

Keywords: geochemical composition; influencing factors; human health risk; absolute principal component score–multiple linear regression; oasis soil; arid central Asia

1. Introduction

Anthropogenic modifications of the natural environment have become more prevalent over the past century and have altered the structure and functional relationships of different ecosystems at a range of scales [1–3]. Soil is the foundation of sustainable agricultural development [4,5], and soil quality has significant effects on human health. Therefore, it is understandable that the amount of pedological research has increased rapidly in recent decades [6,7]. With population growth and economic development, soil environmental problems in many countries have become increasingly prominent [8–10]. Among soil's geochemical components, potentially toxic elements (PTEs) are the main pollutants in farmland soils [11,12]. The pollution from PTEs in farmland soil is related to the quality and safety of agricultural products and the health of farmland ecosystems [13] and has attracted wide attention from governments and scientists of various countries.

PTEs are affected by both the natural environments in which they form and the degree of influence from anthropogenic activity [14,15]. There are many existing models and methods for the apportionment of soil pollution sources, including multivariate statistical methods [16], isotope tracing methods [17,18], receptor models of positive matrix factorization (PMF) [19–21], the chemical mass balance (CMB) model [22], and absolute principal component score–multiple linear regression (APCS-MLR) [23]. The multivariate statistical method qualitatively determines the sources of certain PTEs by identifying PTEs with similar distribution characteristics. The isotope tracing method uses the differences in the isotope ratios of PTEs from different sources to identify the sources and their contributions. Understanding the sources of PTEs polluting the soil, in order to formulate and adopt corresponding source reduction and prevention measures, is a fundamental measure necessary to protect the quality of farmland soil and the safety of agricultural products [24].

Xinjiang Province is an important agricultural base in China; since its establishment in the 1950s, agricultural production in the area has developed considerably. Oasis agriculture is the main farming technique used in arid regions of China [25]. Most oases are located in the piedmont zone, where there is sufficient water supply [26–28]. Although much pedological research has focused on land use [29–31], soil salinization [32,33], and oasis evolution [34] in oasis regions and PTE pollution in coal mining areas [35], such as the southern margin of Tarim Basin [36], Yanqi County [37], and Bosten Lake Watershed [38], few studies have investigated the geochemical composition and PTE concentrations in soils from oasis agricultural regions. Even basic quantitative data are lacking on the impacts of anthropogenic influences on PTE variations in oasis soils over the past decades. The scientific question of this study is as follows: Under the influence of high-intensity human activities, have the potentially toxic elements in the soil changed significantly, and are the types of PTE pollution in the soils of different regions spatially consistent or heterogeneous?

To quantify whether high-intensity exploitation in Xinjiang, China, has commensurately affected the PTE composition and soil quality in the region, we present data from soil surveys of the PTE compositions of surface soils (0–20 cm in depth) from two major oases (the Yili River Watershed and Bortala River Watershed). Using multivariate statistical methods and the APCS-MLR model, the characteristics of PTEs and the differences in their responses to social and economic development are explored in the soils of different geographic units in the piedmont zone of the Tianshan Mountains. This research is expected to provide support for advancing ecological and environmental protection in Xinjiang, China.

2. Materials and Methods

2.1. Sample Collection and Analysis

In July 2018, soils were collected from the irrigated croplands in two oasis regions (Yili River Watershed and Bortala River Watershed) on the slopes of the Tianshan Mountains, Xinjiang Uygur Autonomous Region of China (Figure 1). The soil-sample collection localities are shown in Figure 1 for Bortala River Watershed (E01–E29) and Yili River Watershed (H01–H39). Each sample was a bulked composite of five sub-samples taken as a 10 × 10 m block using the diagonal sampling method [39–41]. According to the Global Soil Maps and Databases from the FAO soils portal (<https://www.fao.org/soils-portal/data-hub/en/>, accessed on 20 August 2021) and the international standard soil classification (World Reference Base for Soil Resources, WRB), the soils in Bortala River Watershed (E01–E29) are Leptosols and Regosols (LP); for the Yili River Watershed, soils H01–H16 are Cambisols (CM), while the others are Leptosols and Regosols (LP) (H17–H39). Soil samples used for geochemical analyses were collected from a 0–20 cm depth at each locality. After air-drying, each composite sample was split into two subsamples, which were then extracted by quartering, a technique that homogenizes a sample by thoroughly mixing it, dividing it into four parts, and retaining two opposite quarters. The measurement of soil grain size is based on our previously published paper [42,43]. According to the classification standard of soil grain size [44], a recalculation was carried out, and the contents for sand (0.05 to 2.0 mm), silt (0.002 to 0.05 mm) and clay (<0.002 mm) was collected. The analysis

of soil organic matter content is determined by the loss-on-ignition method [45]. The pH is measured by the potentiometric method using a suspension of soil and distilled water with a soil-to-water ratio of 1:5 [46,47]. Bulk sediments were dried at 105 °C, ground through a 200 µm mesh, digested with HF–HNO₃–HClO₄ in a MWS-3 microwave digester (Berghof, Eningen, Germany) and prepared for geochemical analysis using a Profile inductively coupled plasma spectrometer (ICP-AES, Leeman Labs, Hudson, NH, USA). To ensure the data quality of the PTEs, blanks, duplicates and standard samples (China national standard soil samples, GBW0731) were set during the determination process. The detection limits for Fe, V, Cr, Co, Ni, Cu, Zn, As, Cd, and Pb were, respectively, 5, 2, 0.1, 0.01, 0.05, 0.02, 0.2, 0.1, 0.01, and 0.02 mg kg⁻¹. The standard solutions for China national standard soil samples (GBW0731) were repeated 11 times, and the recovery was 99.1–101.5%. Duplicates were randomly selected as parallel samples, and the deviation of the measurement results of parallel samples was less than 5%.

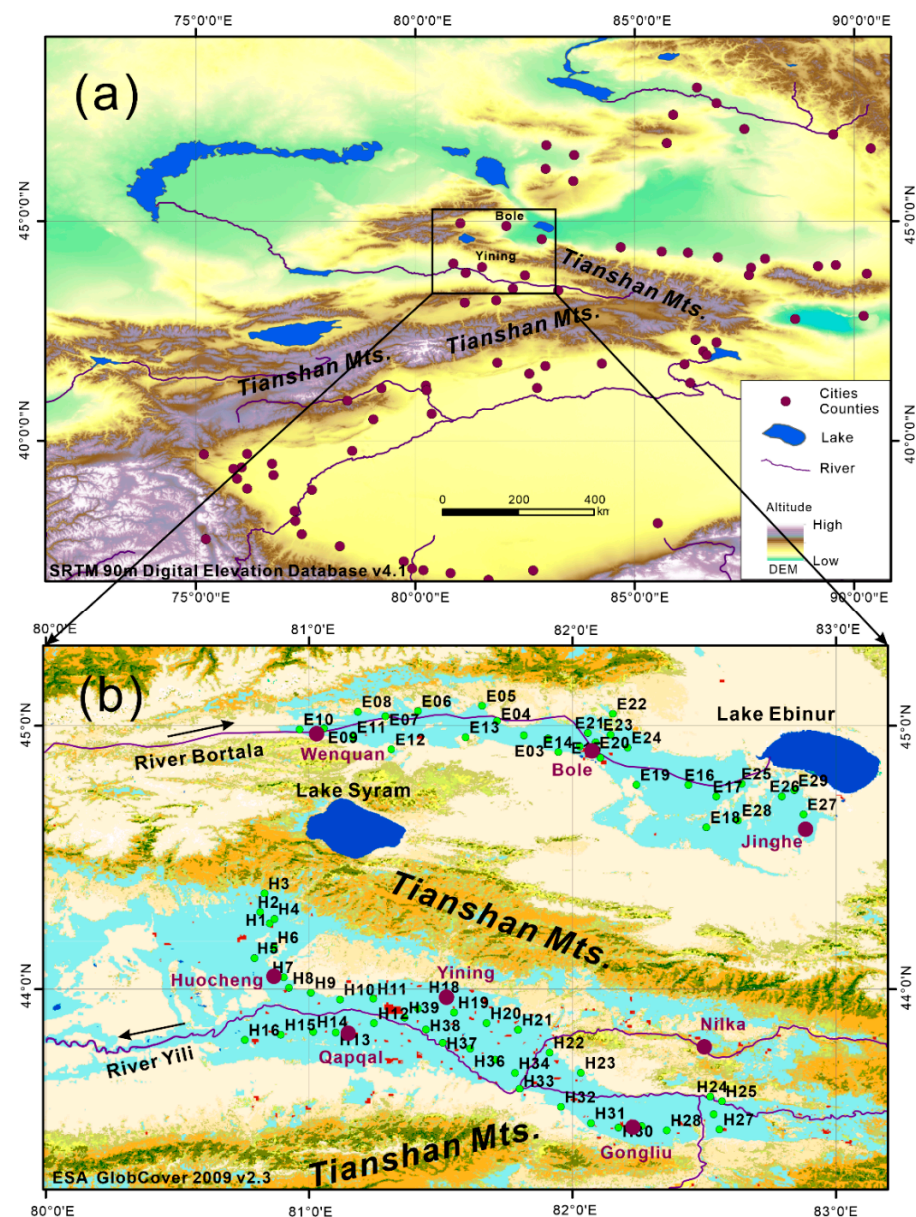


Figure 1. Study area on the slopes of the Tianshan Mountains (a) and the distribution of sampling sites in the Bortala River Watershed (E01–E29) and Yili River Watershed (H01–H39) (b).

2.2. Multivariate Statistical Analysis

A two-way cluster analysis can group different features into significant sets [48,49]. For the cluster analysis, elemental contents were transformed via z-score standardization, $z = (X - \mu) / \sigma$, where z is the z-score, X is the elemental content, μ is the mean value of the elemental contents, and σ is the standard deviation. The nearest-neighbor cluster method using Pearson's correlation distance was utilized for cluster analysis. Factor analysis was conducted for the possible influencing factors of PTEs [50–52]. The optimal cluster number was determined with the elbow method [53,54], and the linear fitting method was used to explore the possible relationship between PTEs and natural background elements [55]. Statistical methods for analyzing surface soil data were conducted using the software OriginPro 2022 learning edition (OriginLab, Northampton, MA, USA).

2.3. The Model of Absolute Principal Component Score–Multiple Linear Regression (APCS-MLR)

Quantitative analysis of pollution sources is an important basis for the environmental management of watershed soils, and the APCS-MLR model was used to obtain the degree of contribution from different material sources to potentially toxic elements in the soil. The APCS-MLR method was based on previously published articles [56–60]. The measured content, C , for PTEs was used as the dependent variable, and the absolute principal component (APCS) was used as the independent variable to perform the multiple linear regression analysis (for the calculation of APCS, refer to references [36–40]). The regression coefficient was obtained using Equation (1):

$$C_j = \sum_k a_{kj} \cdot \text{APCS}_{kj} + b_j \quad (1)$$

where C_j is the measured content of the potentially toxic element j , a_{kj} represents the regression coefficient between C_j and the material source k , and b_j is the constant term of the multiple linear regression. In this model, $a_{kj} \cdot \text{APCS}_{kj}$ expresses the contribution of the pollution source k to C_j .

2.4. Human Health Risks from PTEs

Methods are widely used for assessing the non-carcinogenic and carcinogenic human health risks of PTEs in soil [61–65]. These methods include the following:

For non-carcinogenic risk:

$$ADD_{ing} = \left(\frac{C \times IngR \times EF \times ED}{BW \times AT} \right) \times 10^{-6} \quad (2)$$

$$ADD_{dermal} = \frac{C \times SA \times AF \times ABS \times EF \times ED}{BW \times AT} \quad (3)$$

$$ADD_{inh} = \frac{C \times InhR \times EF \times ED}{PEF \times BW \times AT} \quad (4)$$

$$HQ = \sum \frac{ADD_x}{RfD_x} \quad (5)$$

For carcinogenic risk:

$$LADD_{ing} = \left(\frac{C \times IngR \times EF \times ED}{BW \times LT} \right) \times 10^{-6} \quad (6)$$

$$LADD_{dermal} = \frac{C \times SA \times AF \times ABS \times EF \times ED}{BW \times LT} \quad (7)$$

$$LADD_{inh} = \frac{C \times InhR \times EF \times ED}{PEF \times BW \times LT} \quad (8)$$

$$CR = \sum (LADD_x \times SF_x) \quad (9)$$

The abovementioned parameters for the health risk assessment of PTEs; the exposure concentrations in the Bortala River Watershed ($C_{Bortala}$, mg kg^{-1}) and Yili River Watershed (C_{Yili} , mg kg^{-1}); the reference doses ($\text{mg kg}^{-1} \text{ day}^{-1}$) for oral (Oral RfD), inhalation (Inhal. RfD), and dermal (Dermal RfD), and the slope factor ($(\text{mg kg}^{-1} \text{ day}^{-1})^{-1}$) for the SF of oral (Oral SF), inhalation (Inhal. SF), and dermal (Dermal SF) delivery methods are shown in Tables 1 and 2.

Table 1. Parameters for the health risk assessment of potentially toxic elements.

Parameters	Description	Units	Value	References
ADD_{ing}	Average daily intake from ingestion	$\text{mg kg}^{-1} \text{ day}^{-1}$		
LDD_{ing}	Average daily intake from dermal contact	$\text{mg kg}^{-1} \text{ day}^{-1}$		
ADD_{dermal}	Average daily intake from inhalation	$\text{mg kg}^{-1} \text{ day}^{-1}$		
ADD_{inh}				
HQ	Non-carcinogenic risk	unitless	HQ < 1, no significant risk; HQ > 1, non-carcinogenic effects may occur.	[61–63]
CR	Carcinogenic risk	unitless	Acceptable/tolerable risk range: 10^{-6} – 10^{-4}	[61–63]
C	Concentration of PTE	mg kg^{-1}	upper limit of the 95% confidence interval for the mean (95% UCL).	[61,65]
IngR	Ingestion rate	mg/day	200	[63]
InhR	Inhalation rate	m^3/day	20	[64]
SA	Skin area available for soil contact	cm^2	5700	[64]
AF	Skin adherence factor	$\text{mg cm}^{-2} \text{ day}^{-1}$	0.2	[61,63]
ABS	Absorption factor	unitless	0.001, for As 0.03	[63–65]
PEF	Particle emission factor	m^3/kg	1.36×10^9	[63,64]
EF	Exposure frequency	day/year	350	[64]
ED	Exposure duration	year	24	[64]
BW	Body weight	kg	60	[64]
AT	Average time	day	ED × 365	[61,64]
LT	Lifetime expressed in days	day	70 × 365	[61]
Rfd	Reference dose	$\text{mg kg}^{-1} \text{ day}^{-1}$	Table 2	[61,65]
SF	Slope factor	$(\text{mg kg}^{-1} \text{ day}^{-1})^{-1}$	Table 2	[61,65]

Table 2. Exposure concentration in Bortala River Watershed ($C_{Bortala}$, mg kg^{-1}) and Yili River Watershed (C_{Yili} , mg kg^{-1}) and the reference dose ($\text{mg kg}^{-1} \text{ day}^{-1}$) for oral (Oral RfD), inhalation (Inhal. RfD) and dermal (Dermal RfD), slope factor ($[\text{mg kg}^{-1} \text{ day}^{-1}]^{-1}$) for SF for oral (Oral SF), inhalation (Inhal. SF) and dermal (Dermal SF).

Element	$C_{Bortala}$	C_{Yili}	Oral RfD	Inhal. RfD	Dermal RfD	Oral SF	Inhal. SF	Dermal SF
As-non canc.	24.1	12.9	3.0×10^{-4}	3.0×10^{-4}	1.23×10^{-4}			
As-cancer	24.1	12.9				1.5	15.1	3.66
Cd-non canc.	0.27	0.25	1.0×10^{-3}	1.0×10^{-3}	1.0×10^{-5}			
Cd-cancer	0.27	0.25					6.3	
Co-non canc.	10.4	10.9	2.0×10^{-2}	5.69×10^{-6}	1.6×10^{-2}			
Co-cancer	10.4	10.9					9.8	
Cr-non canc.	48.1	52.2	3.0×10^{-3}	2.86×10^{-5}	6.0×10^{-5}			
Cr-cancer	48.1	52.2					42.0	
Cu	26.0	24.2	4.0×10^{-2}	4.0×10^{-2}	1.2×10^{-2}			
V	77.8	80.1	7.0×10^{-3}	7.0×10^{-3}	7.0×10^{-5}			
Ni-non canc.	26.8	25.3	2.0×10^{-2}	2.0×10^{-2}	5.4×10^{-3}			
Ni-cancer	26.8	25.3					0.84	
Pb	19.2	20.1	3.5×10^{-3}	3.51×10^{-3}	5.25×10^{-4}			
Zn	82.9	74.0	0.3	0.3	6.0×10^{-2}			

3. Results

3.1. General Features of the Soil Element Contents

The mean values of sand, silt and clay content in the Bortala River Basin were 30.15%, 54.85% and 15%, respectively, while the mean value of soil organic matter was 1.41% and soil pH was 8.34. The mean values of sand, silt and clay content in the Yili River Basin were 25.46%, 56.40% and 18.13%, respectively, while the mean value of soil organic matter was 1.61% and soil pH was 8.28. The distribution of soil texture, pH, and organic matter content of each soil sample was shown in Figures S1 and S2. The descriptive statistics for element concentrations in the surface soil samples are presented in Tables 3 and 4. In these tables, the unit for all elements is milligrams per kilogram. There are some differences between the concentrations of key elements analyzed in the soil samples and those reported for the upper continental crust (UCC) [66]. In terms of the mean value, Fe, V, Cr, Co, Ni, and Cu were relatively depleted in the soils of the study area compared to UCC, while Pb and Zn were relatively enriched; and the elements Cd and As were significantly enriched. Although this phenomenon was observed in both regions, a comparison of the elemental contents of the two regions shows that the As content in the soils of the Bortala River Watershed (with a mean value of 20.03 mg kg⁻¹) was much greater than that in the Yili River Watershed (with a mean value of 12.03 mg kg⁻¹).

Table 3. Descriptive statistical results of the soil elements of irrigated cropland in the Bortala River Watershed compared with the upper continental crust (UCC).

Element	N	Mean	SD	SE	Lower 95% CI of Mean	Upper 95% CI of Mean	Minimum	Median	Maximum	UCC
Fe	29	29,758.03	4858.37	902.18	27,910.01	31,606.05	17,038.54	31,141.56	39,014.14	53,300
V	29	72.87	12.94	2.40	67.94	77.79	38.20	75.80	94.35	97
Cr	29	44.87	8.42	1.56	41.66	48.07	26.86	45.74	64.22	92
Co	29	9.72	1.85	0.34	9.02	10.43	5.50	9.67	13.89	17.3
Ni	29	24.99	4.73	0.88	23.19	26.78	14.27	24.72	36.69	47
Cu	29	24.07	5.02	0.93	22.16	25.98	15.57	25.09	32.67	28
Zn	29	77.36	14.65	2.72	71.79	82.93	43.88	77.53	107.74	67
As	29	20.03	10.62	1.97	15.99	24.07	11.97	16.71	61.81	4.8
Cd	29	0.24	0.09	0.02	0.21	0.27	0.13	0.22	0.54	0.09
Pb	29	17.93	3.32	0.62	16.67	19.19	9.75	18.35	25.78	17

Table 4. Descriptive statistical results of the soil elements of irrigated cropland in the Yili River Watershed.

Element	N	Mean	SD	SE	Lower 95% CI of Mean	Upper 95% CI of Mean	Minimum	Median	Maximum	UCC
Fe	39	29,674.33	2951.28	472.58	28,717.64	30,631.03	22,661.35	29,592.25	35,380.00	53,300
V	39	77.53	7.90	1.26	74.97	80.09	56.61	77.94	91.42	97
Cr	39	50.01	6.69	1.07	47.84	52.18	31.94	49.94	61.83	92
Co	39	10.43	1.47	0.24	9.95	10.91	7.61	10.25	12.82	17.3
Ni	39	24.00	3.93	0.63	22.73	25.28	15.71	24.00	30.94	47
Cu	39	22.72	4.41	0.71	21.29	24.15	13.20	22.18	31.77	28
Zn	39	70.38	11.25	1.80	66.73	74.02	47.98	69.74	93.91	67
As	39	12.03	2.58	0.41	11.19	12.86	6.98	11.66	17.73	4.8
Cd	39	0.23	0.05	0.01	0.22	0.25	0.12	0.23	0.35	0.09
Pb	39	19.10	2.20	0.35	18.38	19.81	14.25	19.28	23.12	17

3.2. Cluster Types for the Soil Samples and the PTEs

The cluster analysis results are shown in Figure 2. Here, polar heatmaps reflect the degree of similarity between each element and were applied to determine whether underlying relationships existed between the concentrations of different elements. Based on the optimal cluster number determination (Figure S3), four assemblages were in-

cluded in the dendrogram for the cluster analysis of the PTEs in the Bortala River Watershed (Figures 2a and S3a) and three major clusters were included for the PTEs in the Yili River Watershed (Figures 2b and S3b). For the PTEs in the soil of the Bortala Watershed (Figure 2a), the first clustering category was As; the second category was Cd; the third category was Cu; and the fourth cluster was Pb, Zn, Ni, Co, Cr, and V. For the PTEs in the soil of the Yili River Watershed, the first cluster was As and the second was Cd, which is consistent with the clustering characteristics of PTEs in the soil of the Bortala River Watershed. However, in the Yili River Watershed (Figure 2b), the third category was Pb, Zn, Cu, Co, Ni, Cr, and V, which was significantly different from the soil in the Bortala River Watershed. The element cluster analysis reflects the differences and commonalities between the different regions.

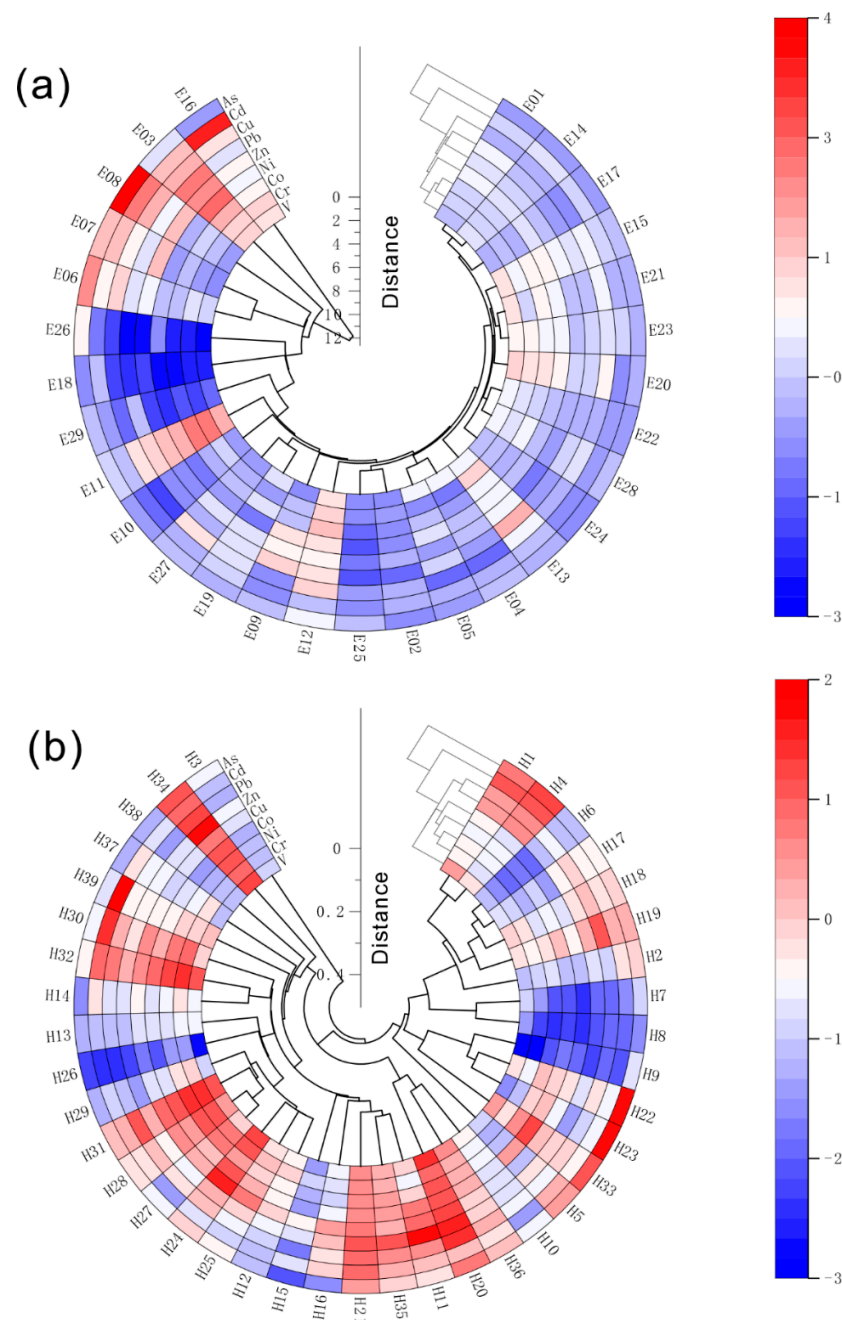


Figure 2. Cluster analysis for the potentially toxic elements and soil samples in the Bortala River Watershed (a) and Yili River Watershed (b) with polar heatmaps and a z-score standardized legend.

The content of PTEs in the cluster analysis was subject to Z-score standardization. Consequently, the distribution of extreme values of the elements can be visualized intuitively from the polar heatmaps. For example, for PTEs in the soil of the Bortala River Watershed, the As contents of the three sample points E6, E7, and E8 were the highest among all samples. For the two samples of E26 and E28, the contents of PTEs in the fourth cluster group (Pb, Zn, Ni, Co, Cr, and V) were the smallest. At the same time, the potentially toxic elements in the soil of the Bortala River Watershed exhibited obvious differences between the first and second cluster group elements (As and Cd) and the fourth cluster group elements (Pb, Zn, Ni, Co, Cr, and V; e.g., at E6, E7, E8, etc). For the soils in the Yili River Watershed, the content of potentially toxic elements in the different clusters of the soil generally showed synergistic changes, which was different from the results in the Bortala River Watershed. For example, at H34, H30, H32, H31, H28, H27, H24, H21, H35, H11, H20, H36, H1, H4, and other samples, the content of the first cluster element (As) was high as were the contents of the third cluster elements (Pb, Zn, Cu, Co, Ni, Cr, and V). In addition, based on the distance of the sample clustering in Figure 2, the differences between soil samples in the Bortala River Watershed were larger than the differences between those in the Yili River Watershed. The above phenomenon indicates that common factors affect the contents of potentially toxic elements in the two regions but that differences also exist.

3.3. Principal Component Analysis Results

Studies have shown that principal component analysis (PCA) has significant advantages in distinguishing the main sources of soil elements [67–69]. Through principal component analysis and calculations, all information on the nine PTEs (nine variables) in the soils of the Bortala River Watershed were reflected by two principal components, with 82.9% total variance (component 1 and 2, Figure 3a); i.e., analysis of the first two components was able to reflect most of the information for all the data. The contribution rate of the first principal component was 63.8%, which was characterized by the higher positive loads of the factor variables on the concentrations of V (0.836), Cr (0.896), Co (0.947), Ni (0.0.845), Cu (0.850), Zn (0.883), and Pb (0.886). However, smaller loadings were observed for As (0.227) and Cd (0.520). The first principal component clearly dominated sources of the PTEs V, Cr, Co, Ni, Cu, Zn, and Pb in the soils. The contribution rate of the second principal component was 19.1%, and the loads of As and Cd were 0.862 and 0.644, respectively. Therefore, the second principal component characterized the source contributions of the PTEs Cd and As in the soils.

In the Yili River Watershed, complete information on the nine PTEs (V, Cr, Co, Ni, Cu, Zn, As, Cd, and Pb) in the soils was also reflected by the two principal components (components 1 and 2, Figure 3b), with 84.5% total variance. The contribution of the first principal component (component 1) was 74.1% and was characterized by a high positive loading of the factor variables on the concentrations of V (0.923), Cr (0.869), Co (0.936), Ni (0.926), Cu (0.887), Zn (0.886), As (0.604), Cd (0.733), and Pb (0.923). The first principal component was the dominant source of PTEs in the soils. The contribution of the second principal component was 10.4%, and the loadings on As and Cd were 0.649 and 0.334, respectively. Thus, the second principal component partly dominated the PTEs As and Cd in the soils.

The PCA results showed some differences between the sources of potentially toxic elements in the soils of the Bortala and Yili river watersheds. Although all nine PTEs were controlled by two sources, control of the primary material source of PTEs was greater in the Yili River Watershed than in the Bortala River Watershed.

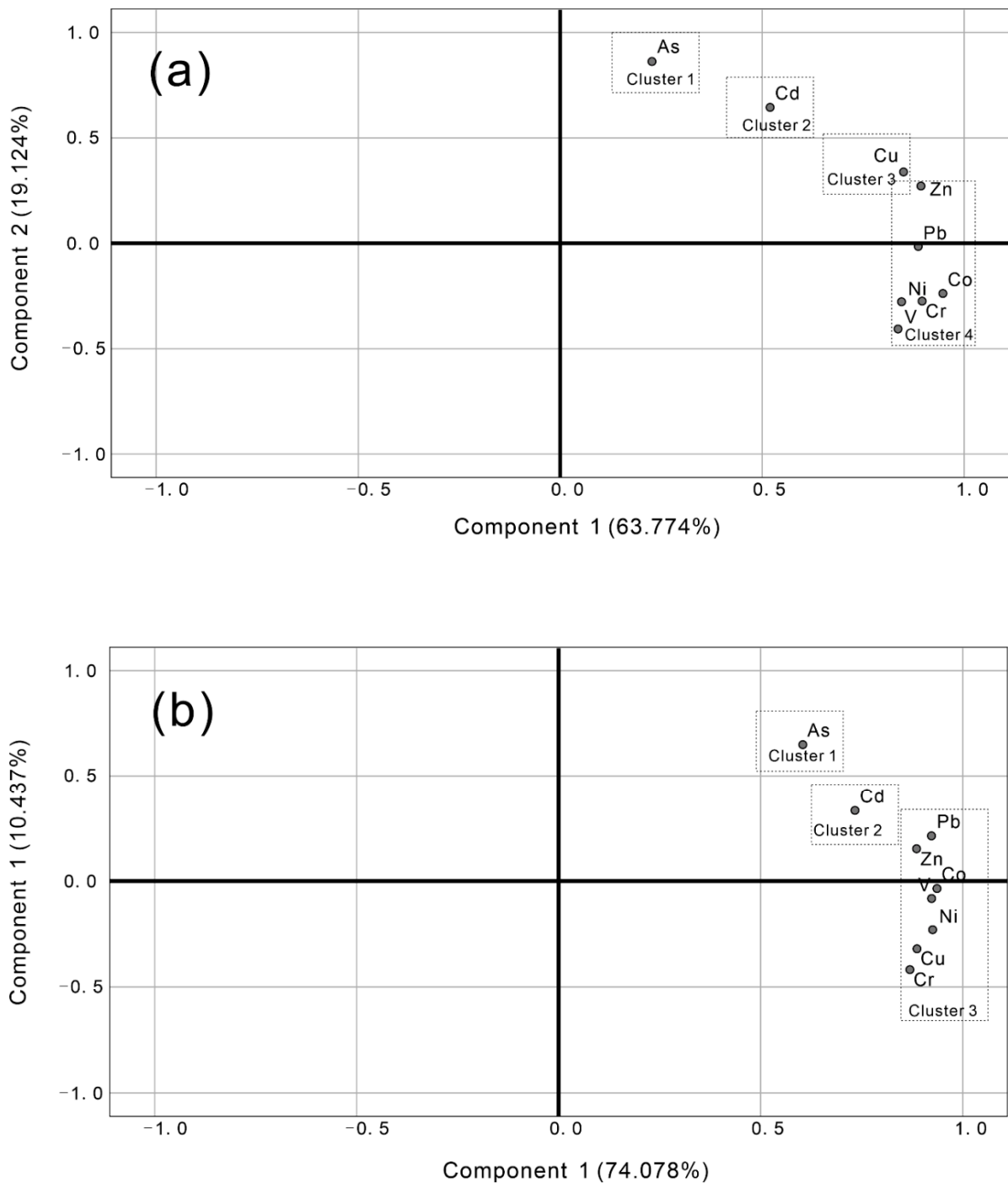


Figure 3. Loading plots of the potentially toxic elements for the principal components in the Bortala River Watershed (a) and Yili River Watershed (b). Clusters 1–3 were derived from the polar heatmaps presented in Figure 2.

3.4. Human Health Risks for PTEs

According to the results of the non-carcinogenic health risk assessment of PTEs in the soil of the Bortala River Watershed (Table 5), As had the largest non-carcinogenic health risk (0.363), but this risk was not significant [61–63]. The health risk ranking of the considered PTEs was As > Cr > V > Pb > Ni > Cu > Co > Cd > Zn. Among these PTEs, As, Cd, Co, Cr, and Ni were the only five PTEs that had potential carcinogenic risks. As had the highest potential carcinogenic risk, with 5.61×10^{-5} . This value falls between 10^{-4} and 10^{-6} , which is an acceptable risk level for carcinogenesis [61–63].

Table 5. Non-carcinogenic (HQ, HI) and carcinogenic risks (RISK) for potentially toxic elements (PTEs) in the Bortala River Watershed and Yili River Watershed.

Region	PTE	HQ _{ing}	HQ _{inh}	HQ _{dermal}	HI = Σ HQ _i	RISK
Bortala	As-non.	0.256	1.89×10^{-5}	0.107	0.363	
	As-canc.	3.96×10^{-5}	2.93×10^{-8}	1.65×10^{-5}		5.61×10^{-5}
	Cd-non.	8.72×10^{-4}	6.41×10^{-8}	4.97×10^{-4}	1.37×10^{-3}	
	Cd-canc.		1.39×10^{-10}			1.39×10^{-10}
	Co-non.	1.67×10^{-3}	4.31×10^{-4}	1.19×10^{-5}	2.11×10^{-3}	
	Co-canc.		8.23×10^{-9}			8.23×10^{-9}
	Cr-non.	5.12×10^{-2}	3.95×10^{-4}	1.46×10^{-2}	6.62×10^{-2}	
	Cr-canc.		1.63×10^{-7}			1.63×10^{-7}
	Cu	2.08×10^{-3}	1.53×10^{-7}	3.94×10^{-5}	2.12×10^{-3}	
	V	3.55×10^{-2}	2.61×10^{-6}	2.02×10^{-2}	5.58×10^{-2}	
	Ni-non.	4.26×10^{-3}	3.13×10^{-7}	9.00×10^{-5}	4.35×10^{-3}	
	Ni-canc.		1.81×10^{-9}			1.81×10^{-9}
	Pb	1.75×10^{-2}	1.29×10^{-6}	6.66×10^{-4}	1.82×10^{-2}	
	Zn	8.84×10^{-4}	6.50×10^{-8}	2.52×10^{-5}	9.09×10^{-4}	
	Yili River	As-non.	0.137	1.01×10^{-5}	5.71×10^{-2}	1.94×10^{-1}
As-canc.		2.11×10^{-5}	1.56×10^{-8}	8.82×10^{-6}		3.00×10^{-5}
Cd-non.		7.99×10^{-4}	5.88×10^{-8}	4.55×10^{-4}	1.25×10^{-3}	
Cd-canc.			1.27×10^{-10}			1.27×10^{-10}
Co-non.		1.74×10^{-3}	4.51×10^{-4}	1.24×10^{-5}	2.21×10^{-3}	
Co-canc.			8.62×10^{-9}			8.62×10^{-9}
Cr-non.		5.56×10^{-2}	4.29×10^{-4}	1.58×10^{-2}	7.19×10^{-2}	
Cr-canc.			1.77×10^{-7}			1.77×10^{-7}
Cu		1.93×10^{-3}	1.42×10^{-7}	3.67×10^{-5}	1.97×10^{-3}	
V		3.66×10^{-2}	2.69×10^{-6}	2.08×10^{-2}	5.74×10^{-2}	
Ni-non.		4.04×10^{-3}	2.97×10^{-7}	8.53×10^{-5}	4.13×10^{-3}	
Ni-canc.			1.71×10^{-9}			1.71×10^{-9}
Pb		1.81×10^{-2}	1.33×10^{-6}	6.87×10^{-4}	1.88×10^{-2}	
Zn		7.89×10^{-4}	5.80×10^{-8}	2.25×10^{-5}	8.11×10^{-5}	

For the Yili River Watershed (Table 5), arsenic also had the largest non-carcinogenic health risk, with 0.194, and reflected no significant risk. The difference between the river watersheds of Yili and Bortala in their health risk rankings of the other PTEs was small and was mainly reflected in the order of Co and Cu. The ranking in the Yili River Watershed was As > Cr > V > Pb > Ni > Co > Cu > Cd > Zn. Arsenic had the highest potential carcinogenic risk with 3.0×10^{-5} . This value falls between 10^{-4} and 10^{-6} , which is also an acceptable risk level for carcinogenesis.

Judging from the level of non-carcinogenic health risks caused by all PTEs, the Bortala River Watershed presents a greater risk than the Yili River Watershed. The total non-carcinogenic risk of the Bortala River Watershed was 0.514 (Total HI in Table 5), whereas that of the Yili River Watershed was 0.352 (Total HI in Table 5). The carcinogenic risk of As in the soil of the Bortala River Watershed was 1.87 times that of the Yili River Watershed.

4. Discussion

In the two sampling areas, the content of the major element Fe was about 30 g kg^{-1} . Due to its high content, Fe is generally not affected by human activities. In a large number of studies, Fe was used as a reference element to study the impacts of human activities on potentially toxic elements relative to natural background levels [70–72]. Potentially toxic elements in soils originate partly from the weathering of bedrock and partly from the contamination of soils by human activities. By establishing the functional relationship between potentially toxic elements and the natural background element Fe, the degree of influence from each potentially toxic element controlled by natural factors can be explored. For the Bortala River Watershed, the coefficients of determination for the linear fitting equation were 78%, 70%, 84%, 63%, 73%, and 65% for V, Cr, Co, Ni, Pb, and Zn, respectively

(Figure 4). These values suggested that natural effects control the variation in these PTEs. Therefore, component 1 in the PCA was set as natural effects (Figure 3). However, the coefficients of determination for Cu, Cd, and As were only 42%, 8%, and 0.7%, respectively (Figure 4). In other words, the influence of human activities on these potentially toxic elements was significant and has altered the characteristics of the potentially toxic elements in their natural context. Therefore, component 2 was determined to be anthropogenic factors (Figure 3). For the Yili River Watershed, the coefficients of determination for the linear fitting equation were 88%, 64%, 70%, 77%, 62%, 66%, and 73%, respectively, for V, Cr, Ni, Co, Cu, Zn, and Pb in the soils (Figure 5). The national soil pollution survey bulletin showed that the five inorganic elements Cd, Hg, As, Cu, and Pb were the primary pollutants in the soils of China [73]. Through our research, we also found that the As, Cd, and Cu levels in the soils of the Bortala River Watershed were significantly affected by human activities and the As and Cd contents in the soils of the Yili River Watershed were found to be strongly affected by human activities among the whole PTEs (V, Cr, Co, Ni, Pb, Zn, Cu, Cd, As). Compared to the soil in the Bortala River Watershed with the coefficients of determination of 8.5% and 0.7% for Cd and As, respectively (Figure 4), the coefficients of determination for the linear fitting equation for Cd and As in the Yili River watershed were 35%, and 39%, respectively (Figure 5). Thus, it suggested that the influences of human activities on PTEs in the Yili River were much stronger than those in the Bortala River watershed.

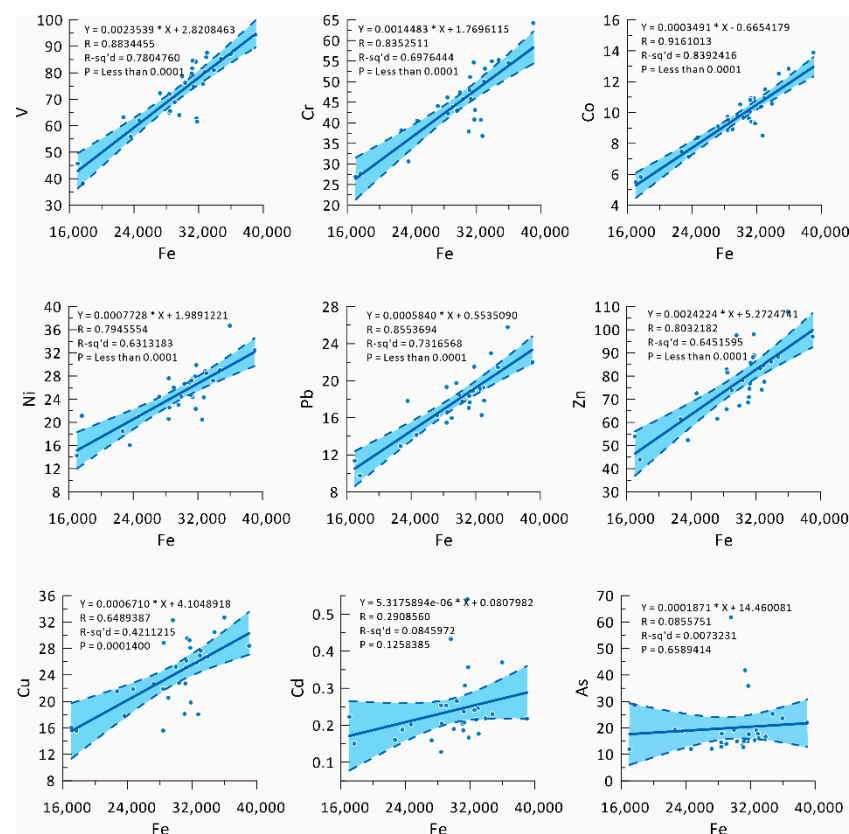


Figure 4. Linear fitting curves of potentially toxic elements in the soils of the Bortala River Watershed and the natural background element Fe.

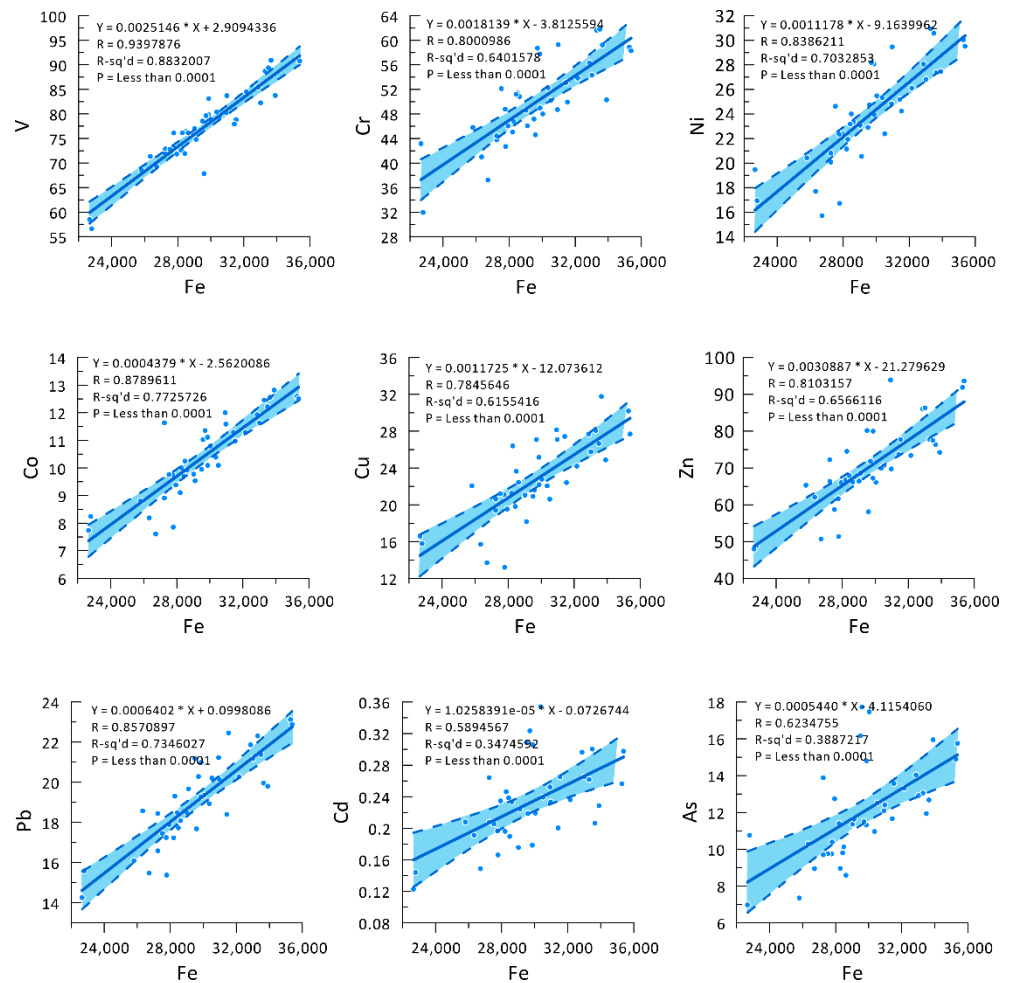


Figure 5. Linear fitting curves of potentially toxic elements in the soils of the Yili River Watershed and the natural background element Fe.

To quantitatively evaluate the influence of human activities on potentially toxic elements, the APCS-MLR model was used to calculate the degree of impact from each potentially toxic element. The fractions of potentially toxic elements V, Cr, Co, Ni, Pb, Zn, Cu, Cd, and As in the soils of the Bortala Basin that originated from human activities were 12%, 6%, 14%, 8%, 17%, 27%, 33%, 64%, and 76%, respectively. On average, the three PTEs Cu, Cd, and As were most strongly affected by human activities, which is consistent with the results of the cluster analysis. The percentages of human sources and natural sources for As, Cd, and Cu at each point are shown in Figure S4. The three sites with the highest As contents (E6, E7, and E8, as shown in the polar heatmap (Figure 2)) were also the most strongly affected by human activities, reaching 82%, 84%, and 89%, respectively.

The potentially toxic elements V, Cr, Ni, Co, Cu, Zn, Pb, Cd, and As in the soils of the Yili River watershed were derived from human activities, accounting for 4%, 10%, 10%, 24%, 21%, 22%, 25%, 40%, and 59%, respectively. Based on the mean values, the two potentially toxic elements Cd and As were the most strongly affected by human activities (cluster 1 and cluster 2 in the cluster analysis (Figure 2)). Unlike in the Bortala River Watershed, the high values of the potentially toxic elemental As in the soils of the Yili River Watershed were not necessarily high due to exposure to human activities. For example, the points with the maximum values of arsenic are H22 and H23 in the cluster analysis diagram (Figure 2), but the point most affected by human activities is H09 (Figure S5), reaching 72%. At the same time, H09 is also the point where Cd was most affected by human activities. In this paper, we investigated the change trends of potentially toxic elements relative to their natural occurrences by considering the soil as a whole and using

elemental Fe as a background element. The physicochemical properties of the soils (e.g., grain size [74], pH [75], total organic matter [76], etc.) will have a direct impact on the distribution and transport of these elements. Correlation analysis shows that the correlation between PTEs and the above-mentioned physical and chemical indicators is not significant (Tables S1 and S2), reflecting the complexity of the factors affecting the content of PTEs in the soil of the study area. In this work, we identified that PTEs such as As and Cd are subject to human activities. The next step will be to investigate the transport patterns of these potentially toxic elements in different physicochemical soil contexts.

Toxicity studies of potentially toxic elements should focus on the chemical forms of PTEs that are strongly related to bioavailability [77,78]. However, the health risk evaluation model for total contents, which is widely used in academia [79,80] and was adopted in this paper, can provide a preliminary evaluation of the contamination status of potentially toxic elements in a holistic manner. Among all the pollutants in the Bortala and Yili River Watersheds, arsenic was determined to be the most serious. Arsenic is a metalloid with high carcinogenic risk, and high contents of arsenic (As) in the natural environment can pose a direct health threat to both humans and ecosystems. In addition to natural causes such as rock weathering, atmospheric arsenic pollution mainly comes from industrial production, the use of arsenic-containing pesticides and phosphate fertilizers, and the burning of coal. Arsenic-containing wastewater can also pollute the soil [81]. Due to the limitations of our current information, we are still unable to give the exact sources of potentially toxic elements and their contributions. Concerning the degree of human health risks in the Bortala River Watershed, increasing the As content to 1.78 times the current level would lead to a risk of cancer. In the Yili River Watershed, ongoing contamination from As in the region alongside an increase in As content to 3.33 times the current level would lead to a risk of cancer. Considering that As itself is a trace element in the Earth's crust, in the Bortala River Watershed and the Yili Basin, the average content is only 20.03 and 12.03 mg kg⁻¹, which should arouse great attention. Thus, arsenic-polluting enterprises in the basin must take effective environmental-protection measures.

According to the social and economic statistics of Xinjiang (Figure 6) the social economy of the Yili Basin and the Bortala Basin has undergone fundamental changes since the 1950s, and both the gross regional product and the total social fixed asset investments have exhibited exponential changes [82]. The development of social economy will inevitably cause environmental pollution. This study shows that two potentially toxic elements, As and Cd, are significantly affected by human activities in both regions. The Bortala River Watershed is significantly greater than the Yili River Watershed in its degree of pollution. However, the land-use intensity (grain production per unit area) and economic development of the Yili River Watershed are significantly greater than the same factors in Bortala, which suggests that the pollution levels of PTEs in Yili River Watershed would be higher than those in the Bortala River Watershed. However, this hypothesis contradicts our actual results. Through the search of relevant literatures, it was found that there were also serious Cd and As pollution in the sediments of the tail lake of the Bortala River [83]. Due to the limitations of our current information, we are still unable to give the exact sources of potentially toxic elements and their contributions. In the future, more in-depth research could be carried out using methods such as source apportionment models [84,85] and isotope tracing [18]. Based on the results of source apportionment in the future, the impact of differences in human social and economic activities on the pollution of PTEs can be objectively and credibility discussed and corresponding control measures will be proposed.

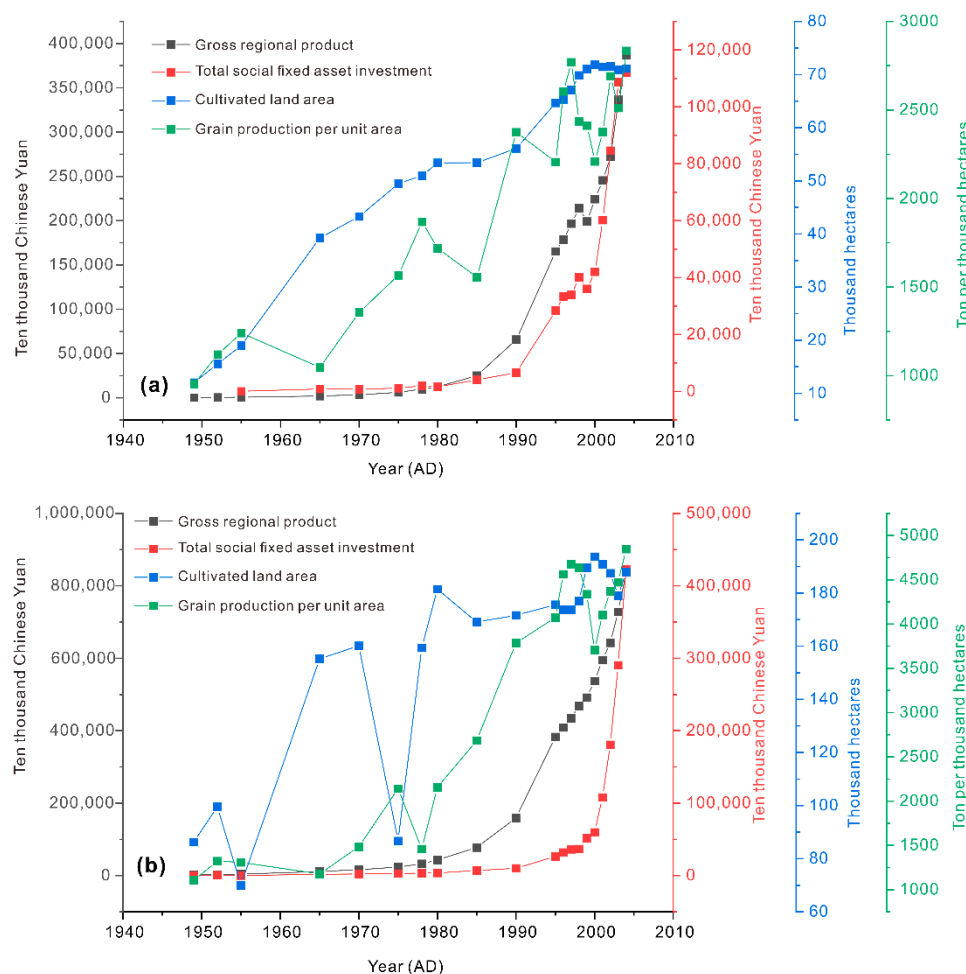


Figure 6. The main social and economic development indicators: gross regional product (unit: ten thousand Chinese Yuan), total social fixed asset investment (unit: ten thousand Chinese Yuan), cultivated land area (unit: thousand hectares), and grain production per unit area (unit: ton per thousand hectares). (a) The Bortala River Watershed, including the three counties of Bole, Jinghe, and Wenquan (locations shown in Figure 1); (b) the Yili River Watershed, including the five counties of Yining, Huocheng, Qapqal, Nilka, and Gongliu (locations shown in Figure 1).

5. Conclusions

- (1) Compared to the upper continental crust (UCC), concentrations of the potentially toxic elements (PTEs) V, Cr, Co, Ni, and Cu were found to be relatively depleted in the oasis agricultural soils in the piedmont zone of the Tianshan Mountains, China. However, Pb and Zn were found to be relatively enriched, and the elements Cd and As were significantly enriched.
- (2) Based on the APCS-MLR model for evaluating the influence of human activities, the PTEs Cd and As in the soils of the Yili River Watershed were found to be the most strongly influenced by human activities, reaching 40% and 59%, respectively. However, in the Bortala River Watershed, Cu, Cd, and As were the most strongly influenced by human activities, reaching 33%, 64%, and 76%, respectively.
- (3) The non-carcinogenic and carcinogenic risks of PTEs on human health are below the threshold. Arsenic represents the largest health risk; this risk should be addressed, and targeted environmental-protection measures should be formulated.

Supplementary Materials: The following are available online at <https://www.mdpi.com/article/10.3390/agriculture11121234/s1>. Figure S1: The soil texture, pH, and soil organic matter (SOM) for sampling sites in the Bortala River Basin. Figure S2: The soil texture, pH, and soil organic matter (SOM) sampling sites in the Yili River Basin. Figure S3: Optimal cluster number determination using the Elbow Method for the Bortala River Watershed (a) and the Yili River Watershed (b). Figure S4: The percentage of anthropogenic and natural sources for As, Cd, and Cu in each sample point in the Bortala River Watershed. Figure S5: The percentage of anthropogenic and natural sources for As and Cd in each sample point in the Yili River Watershed. Table S1: The Pearson correlation for the Potentially toxic elements (PTEs) and soil texture (sand, silt, clay), soil organic matter (SOM) and pH in the soils of Yili River Basin. Table S2: The Pearson correlation for the Potentially toxic elements (PTEs) and soil texture (sand, silt, clay), soil organic matter (SOM) and pH in the soils of Bortala River Basin.

Author Contributions: Conceptualization, L.M.; formal analysis, W.L.; funding acquisition, L.M.; investigation, L.M.; methodology, W.L. and L.M.; supervision, J.A.; visualization, W.L.; writing—original draft, W.L.; writing—review and editing, L.M. and J.A. All authors have read and agreed to the published version of the manuscript.

Funding: This research was funded by National Natural Science Foundation of China (U1903115); the K. C. Wong Education Foundation (GJTD-2020-14); and the High-level Training Project of Xinjiang Institute of Ecology and Geography, CAS (E050030101).

Institutional Review Board Statement: Not applicable.

Informed Consent Statement: Not applicable.

Data Availability Statement: Not applicable.

Acknowledgments: We thank the four anonymous reviewers for their valuable comments and suggestions. We are grateful for the assistance provided by Yingxiao Ge during the field sampling.

Conflicts of Interest: The authors declare no conflict of interest.

References

1. Hooke, R.L.; Martin Duque, J.F.; Pedraza, J. Land transformation by humans: A review. *GSA Today* **2012**, *22*, 4–10. [[CrossRef](#)]
2. Vitousek, P.M.; Mooney, H.A.; Lubchenco, J.; Melillo, J.M. Human domination of Earth's ecosystems. *Science* **1997**, *277*, 494–499. [[CrossRef](#)]
3. Turner, B.L.; Lambin, E.F.; Reenberg, A. The emergence of land change science for global environmental change and sustainability. *Proc. Natl. Acad. Sci. USA* **2007**, *104*, 20666–20671. [[CrossRef](#)]
4. Pang, J.; Liu, X.; Huang, Q. A new quality evaluation system of soil and water conservation for sustainable agricultural development. *Agric. Water Manag.* **2020**, *240*, 106235. [[CrossRef](#)]
5. Lal, R.; Bouma, J.; Brevik, E.; Dawson, L.; Field, D.J.; Glaser, B.; Hatano, R.; Hartemink, A.; Kosaki, T.; Lascelles, B.; et al. Soils and sustainable development goals of the United Nations (New York, USA): An IUSS perspective. *Geoderma Reg.* **2021**, *25*, e00398. [[CrossRef](#)]
6. Abrahams, P.W. Soils: Their implications to human health. *Sci. Total Environ.* **2002**, *291*, 1–32. [[CrossRef](#)]
7. Karlen, D.L.; Andrews, S.S.; Weinhold, B.J.; Doran, J.W. Soil quality: Humankind's foundation for survival. A research editorial by conservation professionals. *J. Soil Water Conserv.* **2003**, *58*, 171–179.
8. Khan, S.; Naushad, M.; Lima, E.C.; Zhang, S.; Shaheen, S.M.; Rinklebe, J. Global soil pollution by toxic elements: Current status and future perspectives on the risk assessment and remediation strategies—A review. *J. Hazard. Mater.* **2021**, *417*, 126039. [[CrossRef](#)]
9. Agyeman, P.C.; Ahado, S.K.; Borůvka, L.; Biney, J.K.M.; Sarkodie, V.Y.O.; Kebonye, N.M.; Kingsley, J. Trend analysis of global usage of digital soil mapping models in the prediction of potentially toxic elements in soil/sediments: A bibliometric review. *Environ. Geochem. Health* **2021**, *43*, 1715–1739. [[CrossRef](#)]
10. Kelepertzis, E. Accumulation of heavy metals in agricultural soils of Mediterranean: Insights from Argolida basin, Peloponnese, Greece. *Geoderma* **2014**, *221*, 82–90. [[CrossRef](#)]
11. Xu, Y.; Dai, S.; Meng, K.; Wang, Y.; Ren, W.; Zhao, L.; Christie, P.; Teng, Y. Occurrence and risk assessment of potentially toxic elements and typical organic pollutants in contaminated rural soils. *Sci. Total Environ.* **2018**, *630*, 618–629. [[CrossRef](#)]
12. Ye, S.; Zeng, G.; Wu, H.; Zhang, C.; Liang, J.; Dai, J.; Liu, Z.; Xiong, W.; Wan, J.; Xu, P. Co-occurrence and interactions of pollutants, and their impacts on soil remediation—A review. *Crit. Rev. Environ. Sci. Technol.* **2017**, *47*, 1528–1553. [[CrossRef](#)]
13. Qin, G.; Niu, Z.; Yu, J.; Li, Z.; Ma, J.; Xiang, P. Soil heavy metal pollution and food safety in China: Effects, sources and removing technology. *Chemosphere* **2021**, *267*, 129205. [[CrossRef](#)]

14. Dung, T.T.T.; Cappuyens, V.; Swennen, R.; Phung, N.K. From geochemical background determination to pollution assessment of heavy metals in sediments and soils. *Rev. Environ. Sci. Bio-Technol.* **2013**, *12*, 335–353. [[CrossRef](#)]
15. McIlwaine, R.; Doherty, R.; Cox, S.F.; Cave, M. The relationship between historical development and potentially toxic element concentrations in urban soils. *Environ. Pollut.* **2017**, *220*, 1036–1049. [[CrossRef](#)] [[PubMed](#)]
16. Zhang, Q.; Zhang, X. Quantitative source apportionment and ecological risk assessment of heavy metals in soil of a grain base in Henan Province, China, using PCA, PMF modeling, and geostatistical techniques. *Environ. Monit. Assess.* **2021**, *193*, 655. [[CrossRef](#)]
17. Liang, X.; Wang, C.; Song, Z.; Yang, S.; Bi, X.; Li, Z.; Li, P. Soil metal(loid)s pollution around a lead/zinc smelter and source apportionment using isotope fingerprints and receptor models. *Appl. Geochem.* **2021**, *135*, 105118. [[CrossRef](#)]
18. Kelepertzis, E.; Argyraki, A.; Chrastrný, V.; Botsou, F.; Skordas, K.; Komárek, M.; Fouskas, A. Metal (loid) and isotopic tracing of Pb in soils, road and house dusts from the industrial area of Volos (central Greece). *Sci. Total Environ.* **2020**, *725*, 138300. [[CrossRef](#)] [[PubMed](#)]
19. Guan, Q.; Wang, F.; Xu, C.; Pan, N.; Lin, J.; Zhao, R.; Yang, Y.; Luo, H. Source apportionment of heavy metals in agricultural soil based on PMF: A case study in Hexi Corridor, northwest China. *Chemosphere* **2018**, *193*, 189–197. [[CrossRef](#)] [[PubMed](#)]
20. Wu, J.; Li, J.; Teng, Y.; Chen, H.; Wang, Y. A partition computing-based positive matrix factorization (PC-PMF) approach for the source apportionment of agricultural soil heavy metal contents and associated health risks. *J. Hazard. Mater.* **2020**, *388*, 121766. [[CrossRef](#)]
21. Zhang, H.; Yin, A.; Yang, X.; Fan, M.; Shao, S.; Wu, J.; Wu, P.; Zhang, M.; Gao, C. Use of machine-learning and receptor models for prediction and source apportionment of heavy metals in coastal reclaimed soils. *Ecol. Indic.* **2021**, *122*, 107233. [[CrossRef](#)]
22. Zhang, H.; Cai, A.; Wang, X.; Wang, L.; Wang, Q.; Wu, X.; Ma, Y. Risk assessment and source apportionment of heavy metals in soils from Handan City. *Appl. Sci.* **2021**, *11*, 9615. [[CrossRef](#)]
23. Wu, J.; Margenot, A.J.; Wei, X.; Fan, M.; Zhang, H.; Best, J.L.; Wu, P.; Chen, F.; Gao, C. Source apportionment of soil heavy metals in fluvial islands, Anhui section of the lower Yangtze River: Comparison of APCS–MLR and PMF. *J. Soils Sediments* **2020**, *20*, 3380–3393. [[CrossRef](#)]
24. Palansooriya, K.N.; Shaheen, S.M.; Chen, S.S.; Tsang, D.C.; Hashimoto, Y.; Hou, D.; Bolan, N.S.; Rinklebe, J.; Ok, Y.S. Soil amendments for immobilization of potentially toxic elements in contaminated soils: A critical review. *Environ. Int.* **2020**, *134*, 105046. [[CrossRef](#)] [[PubMed](#)]
25. Jun, L.; Xiaolei, Z. Structural adjustment of oasis agriculture in Xinjiang. *Chin. J. Popul. Resour. Environ.* **2005**, *3*, 29–33. [[CrossRef](#)]
26. Wei, H.; Liu, H.; Xu, Z.; Ren, J.; Lu, N.; Fan, W.; Zhang, P.; Dong, X. Linking ecosystem services supply, social demand and human well-being in a typical mountain–oasis–desert area, Xinjiang, China. *Ecosyst. Serv.* **2018**, *31*, 44–57. [[CrossRef](#)]
27. Wei, H.; Xu, Z.; Liu, H.; Ren, J.; Fan, W.; Lu, N.; Dong, X. Evaluation on dynamic change and interrelations of ecosystem services in a typical mountain–oasis–desert region. *Ecol. Indic.* **2018**, *93*, 917–929. [[CrossRef](#)]
28. Mamat, A.; Wang, J.; Ma, Y. Impacts of land-use change on ecosystem service value of mountain–oasis–desert ecosystem: A case study of Kaidu–Kongque river basin, Northwest China. *Sustainability* **2021**, *13*, 140. [[CrossRef](#)]
29. Jia, B.; Zhang, Z.; Ci, L.; Ren, Y.; Pan, B.; Zhang, Z. Oasis land-use dynamics and its influence on the oasis environment in Xinjiang, China. *J. Arid. Environ.* **2004**, *56*, 11–26. [[CrossRef](#)]
30. Zhao, R.; Chen, Y.; Shi, P.; Zhang, L.; Pan, J.; Zhao, H. Land use and land cover change and driving mechanism in the arid inland river basin: A case study of Tarim River, Xinjiang, China. *Environ. Earth Sci.* **2013**, *68*, 591–604. [[CrossRef](#)]
31. Abulizi, A.; Yang, Y.; Mamat, Z.; Luo, J.; Abdulslam, D.; Xu, Z.; Zayiti, A.; Ahat, A.; Halik, W. Land-use change and its effects in Charchan Oasis, Xinjiang, China. *Land Degrad. Dev.* **2017**, *28*, 106–115. [[CrossRef](#)]
32. Wang, J.; Liu, Y.; Wang, S.; Liu, H.; Fu, G.; Xiong, Y. Spatial distribution of soil salinity and potential implications for soil management in the Manas River watershed, China. *Soil Use Manag.* **2020**, *36*, 93–103. [[CrossRef](#)]
33. Wang, Y.; Xiao, D.; Li, Y.; Li, X. Soil salinity evolution and its relationship with dynamics of groundwater in the oasis of inland river basins: Case study from the Fubei region of Xinjiang Province, China. *Environ. Monit. Assess.* **2008**, *140*, 291–302. [[CrossRef](#)]
34. Hong, Z.; Jian-Wei, W.; Qiu-Hong, Z.; Yun-Jiang, Y. A preliminary study of oasis evolution in the Tarim Basin, Xinjiang, China. *J. Arid. Environ.* **2003**, *55*, 545–553. [[CrossRef](#)]
35. Zhang, H.; Zhang, F.; Song, J.; Tan, M.L.; Kung, H.-t.; Johnson, V.C. Pollutant source, ecological and human health risks assessment of heavy metals in soils from coal mining areas in Xinjiang, China. *Environ. Res.* **2021**, *202*, 111702. [[CrossRef](#)] [[PubMed](#)]
36. Fan, W.; Zhou, J.; Zhou, Y.; Wang, S.; Du, J.; Chen, Y.; Zeng, Y.; Wei, X. Heavy metal pollution and health risk assessment of agricultural land in the Southern Margin of Tarim Basin in Xinjiang, China. *Int. J. Environ. Health Res.* **2021**, *31*, 835–847. [[CrossRef](#)] [[PubMed](#)]
37. Mamut, A.; Eziz, M.; Mohammad, A. Pollution and ecological risk assessment of heavy metals in farmland soils in Yanqi County, Xinjiang, Northwest China. *Eurasian Soil Sci.* **2018**, *51*, 985–993. [[CrossRef](#)]
38. Ma, L.; Abuduwaili, J.; Liu, W. Spatial distribution and health risk assessment of potentially toxic elements in surface soils of Bosten lake basin, central Asia. *Int. J. Environ. Res. Public Health* **2019**, *16*, 3741. [[CrossRef](#)]
39. Amini, M.; Afyuni, M.; Fathianpour, N.; Khademi, H.; Flühler, H. Continuous soil pollution mapping using fuzzy logic and spatial interpolation. *Geoderma* **2005**, *124*, 223–233. [[CrossRef](#)]
40. Yemefack, M.; Rossiter, D.G.; Njomgang, R. Multi-scale characterization of soil variability within an agricultural landscape mosaic system in southern Cameroon. *Geoderma* **2005**, *125*, 117–143. [[CrossRef](#)]

41. Amusan, A.; Ige, D.; Olawale, R. Characteristics of soils and crops' uptake of metals in municipal waste dump sites in Nigeria. *J. Human Ecol.* **2005**, *17*, 167–171. [[CrossRef](#)]
42. Ma, L.; Wu, J.; Abuduwaili, J. Variation in aeolian environments recorded by the particle size distribution of lacustrine sediments in Ebinur Lake, northwest China. *SpringerPlus* **2016**, *5*, 481. [[CrossRef](#)]
43. Ma, L.; Abuduwaili, J.; Liu, W. Environmentally sensitive grain-size component records and its response to climatic and anthropogenic influences in Bosten Lake region, China. *Sci. Rep.* **2020**, *10*, 942. [[CrossRef](#)]
44. Arshad, M.A.; Lowery, B.; Grossman, B. Physical tests for monitoring soil quality. In *Methods for Assessing Soil Quality*; John Wiley and Sons: Hoboken, NJ, USA, 1997; pp. 123–141.
45. Ma, L.; Wu, J.; Abuduwaili, J. Climate and environmental changes over the past 150 years inferred from the sediments of Chaiwopu Lake, central Tianshan Mountains, northwest China. *Int. J. Earth Sci.* **2013**, *102*, 959–967. [[CrossRef](#)]
46. Bednik, M.; Medyńska-Juraszek, A.; Dudek, M.; Kloc, S.; Kręt, A.; Łabaz, B.; Waroszewski, J. Wheat straw biochar and NPK fertilization efficiency in sandy soil reclamation. *Agronomy* **2020**, *10*, 496. [[CrossRef](#)]
47. Li, X.; Gao, Y.; Zhang, M.; Zhang, Y.; Zhou, M.; Peng, L.; He, A.; Zhang, X.; Yan, X.; Wang, Y.; et al. In vitro lung and gastrointestinal bioaccessibility of potentially toxic metals in Pb-contaminated alkaline urban soil: The role of particle size fractions. *Ecotox. Environ. Safte.* **2020**, *190*, 110151. [[CrossRef](#)] [[PubMed](#)]
48. Swanson, S.K.; Bahr, J.M.; Schwar, M.T.; Potter, K.W. Two-way cluster analysis of geochemical data to constrain spring source waters. *Chem. Geol.* **2001**, *179*, 73–91. [[CrossRef](#)]
49. Iqbal, M.; Khan, S.M.; Azim Khan, M.; Ahmad, Z.; Ahmad, H. A novel approach to phytosociological classification of weeds flora of an agro-ecological system through Cluster, Two Way Cluster and Indicator Species Analyses. *Ecol. Indic.* **2018**, *84*, 590–606. [[CrossRef](#)]
50. Maiz, I.; Arambarri, I.; Garcia, R.; Millán, E. Evaluation of heavy metal availability in polluted soils by two sequential extraction procedures using factor analysis. *Environ. Pollut.* **2000**, *110*, 3–9. [[CrossRef](#)]
51. Ye, C.; Li, S.; Zhang, Y.; Zhang, Q. Assessing soil heavy metal pollution in the water-level-fluctuation zone of the Three Gorges Reservoir, China. *J. Hazard. Mater.* **2011**, *191*, 366–372. [[CrossRef](#)]
52. Uygur, N.; Karaca, F.; Alagha, O. Prediction of sources of metal pollution in rainwater in Istanbul, Turkey using factor analysis and long-range transport models. *Atmos. Res.* **2010**, *95*, 55–64. [[CrossRef](#)]
53. Liu, F.; Deng, Y. Determine the number of unknown targets in Open World based on Elbow method. *IEEE Trans. Fuzzy Syst.* **2020**, *29*, 986–995. [[CrossRef](#)]
54. Yuan, C.; Yang, H. Research on K-value selection method of K-means clustering algorithm. *J. Agric. Saf. Health* **2019**, *2*, 226–235. [[CrossRef](#)]
55. Kumar Sharma, R.; Agrawal, M.; Marshall, F. Heavy metal contamination of soil and vegetables in suburban areas of Varanasi, India. *Ecotox. Environ. Saf.* **2007**, *66*, 258–266. [[CrossRef](#)]
56. Zhang, H.; Cheng, S.; Li, H.; Fu, K.; Xu, Y. Groundwater pollution source identification and apportionment using PMF and PCA-APCA-MLR receptor models in a typical mixed land-use area in Southwestern China. *Sci. Total Environ.* **2020**, *741*, 140383. [[CrossRef](#)]
57. Jin, G.; Fang, W.; Shafi, M.; Wu, D.; Li, Y.; Zhong, B.; Ma, J.; Liu, D. Source apportionment of heavy metals in farmland soil with application of APCS-MLR model: A pilot study for restoration of farmland in Shaoxing City Zhejiang, China. *Ecotox. Environ. Saf.* **2019**, *184*, 109495. [[CrossRef](#)]
58. Shen, D.; Huang, S.; Zhang, Y.; Zhou, Y. The source apportionment of N and P pollution in the surface waters of lowland urban area based on EEM-PARAFAC and PCA-APCS-MLR. *Environ. Res.* **2021**, *197*, 111022. [[CrossRef](#)] [[PubMed](#)]
59. Zhang, W.H.; Yan, Y.; Yu, R.L.; Hu, G.R. The sources-specific health risk assessment combined with APCS/MLR model for heavy metals in tea garden soils from south Fujian Province, China. *Catena* **2021**, *203*, 105306. [[CrossRef](#)]
60. Haji Gholizadeh, M.; Melesse, A.M.; Reddi, L. Water quality assessment and apportionment of pollution sources using APCS-MLR and PMF receptor modeling techniques in three major rivers of South Florida. *Sci. Total Environ.* **2016**, *566–567*, 1552–1567. [[CrossRef](#)] [[PubMed](#)]
61. Ferreira-Baptista, L.; De Miguel, E. Geochemistry and risk assessment of street dust in Luanda, Angola: A tropical urban environment. *Atmos. Environ.* **2005**, *39*, 4501–4512. [[CrossRef](#)]
62. Jiang, Y.; Chao, S.; Liu, J.; Yang, Y.; Chen, Y.; Zhang, A.; Cao, H. Source apportionment and health risk assessment of heavy metals in soil for a township in Jiangsu Province, China. *Chemosphere* **2017**, *168*, 1658–1668. [[CrossRef](#)] [[PubMed](#)]
63. Lu, X.; Zhang, X.; Li, L.Y.; Chen, H. Assessment of metals pollution and health risk in dust from nursery schools in Xi'an, China. *Environ. Res.* **2014**, *128*, 27–34. [[CrossRef](#)]
64. Chabukdhara, M.; Nema, A.K. Heavy metals assessment in urban soil around industrial clusters in Ghaziabad, India: Probabilistic health risk approach. *Ecotox. Environ. Saf.* **2013**, *87*, 57–64. [[CrossRef](#)] [[PubMed](#)]
65. De Miguel, E.; Iribarren, I.; Chacón, E.; Ordoñez, A.; Charlesworth, S. Risk-based evaluation of the exposure of children to trace elements in playgrounds in Madrid (Spain). *Chemosphere* **2007**, *66*, 505–513. [[CrossRef](#)]
66. Rudnick, R.; Gao, S. The crust. In *Treatise on Geochemistry*; Kelemen, P., Hanghøj, K., Greene, A., Eds.; Elsevier: Amsterdam, The Netherlands, 2003; Volume 3.
67. Yang, H.; Wang, F.; Yu, J.; Huang, K.; Zhang, H.; Fu, Z. An improved weighted index for the assessment of heavy metal pollution in soils in Zhejiang, China. *Environ. Res.* **2021**, *192*, 110246. [[CrossRef](#)] [[PubMed](#)]

68. Yang, Y.; Yang, X.; He, M.; Christakos, G. Beyond mere pollution source identification: Determination of land covers emitting soil heavy metals by combining PCA/APCS, GeoDetector and GIS analysis. *Catena* **2020**, *185*, 104297. [[CrossRef](#)]
69. Bern, C.R.; Walton-Day, K.; Naftz, D.L. Improved enrichment factor calculations through principal component analysis: Examples from soils near breccia pipe uranium mines, Arizona, USA. *Environ. Pollut.* **2019**, *248*, 90–100. [[CrossRef](#)]
70. Liu, W.X.; Li, X.D.; Shen, Z.G.; Wang, D.C.; Wai, O.W.H.; Li, Y.S. Multivariate statistical study of heavy metal enrichment in sediments of the Pearl River Estuary. *Environ. Pollut.* **2003**, *121*, 377–388. [[CrossRef](#)]
71. Ustaoglu, F.; Islam, M.S. Potential toxic elements in sediment of some rivers at Giresun, Northeast Turkey: A preliminary assessment for ecotoxicological status and health risk. *Ecol. Indic.* **2020**, *113*, 106237. [[CrossRef](#)]
72. Li, L.; Wu, J.; Lu, J.; Min, X.; Xu, J.; Yang, L. Distribution, pollution, bioaccumulation, and ecological risks of trace elements in soils of the northeastern Qinghai-Tibet Plateau. *Ecotox. Environ. Saf.* **2018**, *166*, 345–353. [[CrossRef](#)]
73. Zhao, F.-J.; Ma, Y.; Zhu, Y.-G.; Tang, Z.; McGrath, S.P. Soil contamination in China: Current status and mitigation strategies. *Environ. Sci. Technol.* **2015**, *49*, 750–759. [[CrossRef](#)] [[PubMed](#)]
74. Wang, X.-S.; Qin, Y.; Chen, Y.-K. Heavy metals in urban roadside soils, part 1: Effect of particle size fractions on heavy metals partitioning. *Environ. Geol.* **2006**, *50*, 1061–1066. [[CrossRef](#)]
75. Zhong, X.; Chen, Z.; Li, Y.; Ding, K.; Liu, W.; Liu, Y.; Yuan, Y.; Zhang, M.; Baker, A.J.; Yang, W. Factors influencing heavy metal availability and risk assessment of soils at typical metal mines in Eastern China. *J. Hazard. Mater.* **2020**, *400*, 123289. [[CrossRef](#)]
76. Stefanowicz, A.M.; Kapusta, P.; Zubek, S.; Stanek, M.; Woch, M.W. Soil organic matter prevails over heavy metal pollution and vegetation as a factor shaping soil microbial communities at historical Zn–Pb mining sites. *Chemosphere* **2020**, *240*, 124922. [[CrossRef](#)]
77. Huang, Z.-Y.; Qin, D.-P.; Zeng, X.-C.; Li, J.; Cao, Y.-L.; Cai, C. Species distribution and potential bioavailability of exogenous Hg (II) in vegetable-growing soil investigated with a modified Tessier scheme coupled with isotopic labeling technique. *Geoderma* **2012**, *189*, 243–249. [[CrossRef](#)]
78. Ahn, Y.; Yun, H.-S.; Pandi, K.; Park, S.; Ji, M.; Choi, J. Heavy metal speciation with prediction model for heavy metal mobility and risk assessment in mine-affected soils. *Environ. Sci. Pollut. Res.* **2020**, *27*, 3213–3223. [[CrossRef](#)]
79. Tepanosyan, G.; Sahakyan, L.; Belyaeva, O.; Maghakyan, N.; Saghatlyan, A. Human health risk assessment and riskiest heavy metal origin identification in urban soils of Yerevan, Armenia. *Chemosphere* **2017**, *184*, 1230–1240. [[CrossRef](#)]
80. Zhao, H.; Xia, B.; Fan, C.; Zhao, P.; Shen, S. Human health risk from soil heavy metal contamination under different land uses near Dabaoshan Mine, Southern China. *Sci. Total Environ.* **2012**, *417–418*, 45–54. [[CrossRef](#)]
81. Garelick, H.; Jones, H.; Dybowska, A.; Valsami-Jones, E. Arsenic pollution sources. In *Reviews of Environmental Contamination: International Perspectives on Arsenic Pollution and Remediation*; Springer: New York, NY, USA, 2008; pp. 17–60.
82. Qiu, Y. *Fifty Years in Xinjiang: 1955–2005*; China Statistics Press: Beijing, China, 2005.
83. Mi, Y.; Chang, S.; Shi, Q.; Gao, X.; Huang, C. Aquatic environmental quality assessment in Ebinur Lake catchment during high flow period. *J. Lake Sci.* **2008**, *21*, 891–894.
84. Huang, Y.; Deng, M.; Wu, S.; Japenga, J.; Li, T.; Yang, X.; He, Z. A modified receptor model for source apportionment of heavy metal pollution in soil. *J. Hazard. Mater.* **2018**, *354*, 161–169. [[CrossRef](#)] [[PubMed](#)]
85. Fei, X.; Lou, Z.; Xiao, R.; Ren, Z.; Lv, X. Contamination assessment and source apportionment of heavy metals in agricultural soil through the synthesis of PMF and GeoDetector models. *Sci. Total Environ.* **2020**, *747*, 141293. [[CrossRef](#)] [[PubMed](#)]